Journal of the Mechanical Behavior of Biomedical Materials 77 (2018) 754–763

Contents lists available at ScienceDirect

Journal of the Mechanical Behavior of Biomedical Materials

journal homepage: www.elsevier.com/locate/jmbbm

Experimental characterization and model identification of the nonlinear compressible material behavior of lung parenchyma

Anna M. Birzle[a,*], Christian Martin[b], Lena Yoshihara[a], Stefan Uhlig[b], Wolfgang A. Wall[a]

[a] Institute for Computational Mechanics, Technical University of Munich, Boltzmannstr. 15, 85747 Garching b. München, Germany
[b] Institute of Pharmacology and Toxicology, RWTH Aachen University, Wendlingweg 2, 52074 Aachen, Germany

ARTICLE INFO

Keywords:
Experimental methods
Numerical Identification
Nonlinear compressibility
Lung parenchyma
Soft tissue mechanics

ABSTRACT

The mechanical properties of lung parenchyma are essential both in lung function and biology; consequently, experimental methods are developed to describe the mechanical behavior of lung parenchyma. During breathing and mechanical ventilation, volume change is the physiologically dominating deformation mode of lung parenchyma; nevertheless, most studies examine lung tissue in mainly isochoric tension tests. In this paper, a novel experimental method for the quantification of the compressible material behavior at high volume changes of viable lung parenchyma is proposed. This volume-pressure-change experiment quantifies the pressure and corresponding volume change of lung parenchyma slices. For the characterization of the compressible constitutive properties over the whole physiological pressure range, we combine this newly derived experiment with uniaxial tension tests. The experimental results of both the volume-pressure-change experiments, for which 287 samples were examined, and the uniaxial tension tests, which were performed on 36 specimens, are presented. The resulting measurements are utilized to optimize the material parameters of one suitable hyperelastic strain-energy function describing the nonlinear compressible material behavior of viable lung parenchyma. The derived constitutive model can be used for simulations of lung parenchyma, and will help to quantify the strains and stresses of lung tissue during normal breathing and mechanical ventilation.

1. Introduction

Characterizing the compressible material properties of lung tissue is an essential ingredient allowing the description and prediction of the mechanical behavior and injury of lung parenchyma during normal and artificial breathing. To better understand lung mechanics in health and disease and to improve therapeutic approaches, global and continuum mechanics based models of the whole respiratory system have been developed. Global models, as for example pressure-volume curves of whole lungs, are not able to describe the underlying phenomena in the respiratory system. In contrast, consider continuum models the individual effects and mutual interaction of lung parenchyma, surfactant, airways, and air flow (see e.g., Berger et al., 2015; Roth et al., 2017; Wall et al., 2010). This separation of the different mechanical phenomena should allow the simulation and even prediction of the progress of several lung diseases, as well as the effects of different interventions. For instance, improper mechanical ventilation can locally overstrain lung tissue and cause ventilator-associated lung injury (VALI) (Consensus-Conference, 1999), particularly in the case of patients suffering from pre-existing lung injuries, such as the acute respiratory distress syndrome (ARDS) (Ware and Matthay, 2000). Continuum mechanics based lung models can provide insights into involved phenomena and support the development of protective ventilation strategies. For these lung models and to better understand the mechanical behavior of lung tissue, an accurate description of the constitutive continuum mechanics model of lung parenchyma is essential. In this paper, the material behavior of the tissue itself without surfactant and airways is characterized, because the mechanical properties of surfactant and airways can be modeled separately (e.g., Roth et al., 2017; Wiechert et al., 2009) and are mechanically coupled in our lung model (Yoshihara et al., 2017).

The main function of lung parenchyma is the gas exchange; therefore, the exchange-area is maximized through a foam-like structure, composed of bronchioles (i.e., small airways), alveoli (i.e., small cavities forming the blood-gas barrier) and the enclosed air volume. The major load-bearing elements in lung tissue are collagen and elastin fibers, which are aligned along the alveolar walls (Yuan et al., 2000). However, on a macroscopic scale, the alveolar wall orientations and, consequently, the fiber orientations have no preferred direction (Sobin et al., 1988; Toshima et al., 2004). Hence, lung parenchyma, i.e., the

* Corresponding author.
E-mail address: birzle@lnm.mw.tum.de (A.M. Birzle).

https://doi.org/10.1016/j.jmbbm.2017.08.001
Received 10 May 2017; Received in revised form 26 July 2017; Accepted 2 August 2017
Available online 05 August 2017

homogenized representation of all these constituents and structures, is assumed to behave isotropically, which was also confirmed in a previous study by Hoppin et al. (1975). Further, lung parenchyma is homogeneous (Tai and Lee, 1981).

Pressure-volume change experiments on whole lungs or lung lobes (e.g., Lai-Fook et al., 1976; Neergaard, 1929; Stamenovic and Yager, 1988) describe the mechanical behavior of a mixture of all involved constituents (namely parenchyma, airways, vessels, surfactant and the pleural membrane). Accordingly, these experiments are not suitable for the mechanical characterization of lung parenchyma alone. Alternatively, the mechanical characterization of isolated lung parenchyma can be achieved by deriving the macroscopic, homogenized behavior of the air-tissue mixture from simulations with resolved microstructures (e.g., Budiansky and Kimmel, 1987; Denny and Schroter, 2000; Lanir, 1983). However, various simplifying assumptions regarding the geometry of the microstructure and the mechanical properties of individual alveolar walls have to be made. Due to these assumptions it is not reasonable to use these material models in predictive lung simulations. As a result, performing experiments on excised samples is most suitable for the identification of the mechanical behavior of lung parenchyma alone.

During breathing, the alveoli are inflated with air, leading to high volume changes of the tissue. As a consequence, lung parenchyma is compressible (Lai-Fook, 1977), in contrast to most soft tissues examined and modeled in the literature (e.g., aorta, skin). On an organ scale at the deepest possible expiration, the volume change of human lungs is already approximately at a factor of 3; during the deepest inspiration a volume change of even a factor of 10 occurs (Agostoni and Hyatt, 2011). Hence, a precise model of the compressible properties over the whole physiological volume-change range is essential in the description of the material behavior of lung parenchyma. Nevertheless, most of the previous studies only examine the isochoric nonlinear (visco)elastic behavior of excised samples of lung parenchyma. Consequently, the aim of this study is the mechanical characterization of the compressible properties of lung parenchyma. Most previous studies use uniaxial tension tests on tissue slices; for example, Bel-Brunon et al. (2014); Maksym and Bates (1997); Navajas et al. (1995) and Rausch et al. (2011). Some also examine the material properties by means of uniaxial compression (Andrikakou et al., 2016) or of biaxial tension tests (e.g., Gao et al., 2005; Vawter et al., 1978; Yager et al., 1992). Gao et al. (2005) state, that a biaxial tension test is enough to describe the constitutive equation in three dimensions. But, with a biaxial tension test it is not possible to measure a three-dimensional volumetric deformation state (i.e., large stretches in all three dimensions). As a consequence, the physiologically dominating compressible material properties are not precisely described with these studies.

Just one experiment by Hoppin et al. (1975) exists that examines the compressibility of lung parenchyma in a three-dimensional tension test (the same protocol was also used by Tai and Lee, 1981). However, this approach has some major limitations. First, during preparation, the tissue was frozen, a process that alters the mechanical behavior (Karlinsky et al., 1985). Second, during the test, the tissue was fixed by means of fish hooks; however, these fish hooks distort the tissue locally, and large boundary effects occur. Third, the volume of the reference state and during the experiment was measured by means of approximated projections of photographs. These lines were drawn manually; consequently, a precise measurement of the volume (and the area for the calculation of the stresses) was not possible with this set-up. Finally, just three tissue specimens were examined.

Thus, no experimental method and no measurements exist that adequately describe the compressible material behavior of viable lung parenchyma at high volume changes. The aim of this paper is to fill this gap. Hence, we have developed a novel type of experiment to precisely measure the compressible material properties. Based on our experimental results, a suitable constitutive model for lung parenchyma is chosen and corresponding material parameters are identified.

This paper is divided into five parts: the first part focuses on the experimental methods, particularly on the newly developed volume-pressure-change experiment to measure the compressible material properties at high volume changes. In the second part, the experimental results are detailed. In the third part, the numerical identification of the compressible material model is described. The fourth and fifth parts cover the discussion and conclusion.

2. Experimental testing of precision-cut lung slices

Tissue samples were harvested from female Wistar rats, obtained from Charles River Laboratories (Sulzfeld, Germany). All animal experiments were approved by the local authorities.

2.1. Preparation of PCLS at well-defined pressurized states

For the identification of the compressible material behavior, especially at high volume changes, we prepared viable, precision-cut lung slices (PCLS) at different well-defined pressurized states. First, the chest of the rats were opened directly after death. Due to the open chest, the lungs collapse, and the air in the alveoli streams out. Via the trachea these empty lungs were filled with gelatin (porcine skin type A), dissolved in a minimum essential medium (8% w/v). To determine a precise and static pressure state p_{fill} in the lung parenchyma, the lungs were filled with the help of a certain gelatin column (Fig. 1). The height of the column was measured from the hilus of the lungs. The gelatin column was held, while the lungs were put on ice to allow the gelatin to solidify. Hence, the stress state p_{fill} was fixed in the parenchyma, independent from the further treatment.

The lungs were dissected from the animal, with the lobes then separated and cut into cylinders of 15 mm diameter. With the help of a Krumdieck tissue slicer (Alabama Research and Development, Munford, AL), these tissue cylinders were cut into slices of 0.5–2 mm. The orientation of the sample with respect to the lung is random. The parenchyma of these viable, precision-cut lung slices was present at a well-defined pressure state p_{fill}. For illustrative purposes, Figs. 2a and b show light microscope images of two PCLS at different pressure states. Due to the higher pressure in Fig. 2a, the alveoli are bigger than in Fig. 2b.

To hold the stress state in the tissue, and therefore prevent the gelatin from melting, the PCLS were cooled and kept in an ice-cold minimum essential medium (MEM) until the experiment was

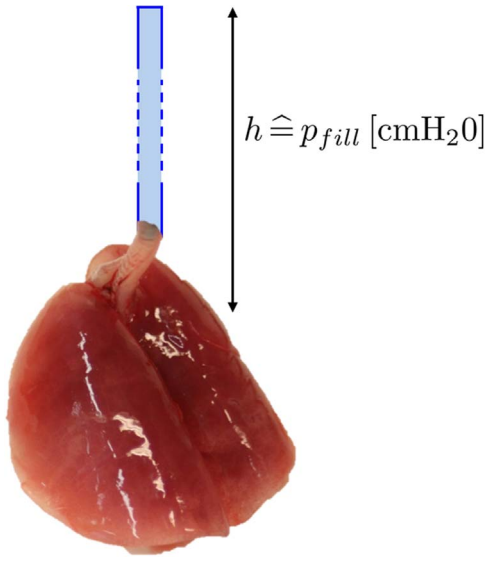

Fig. 1. Schematic set-up of preparation of rat lungs by means of a certain gelatin column to obtain PCLS at a well-defined pressurized state.

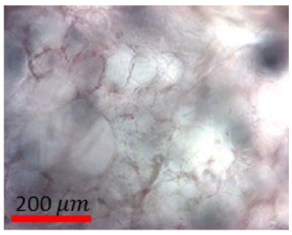

(a) Precision-cut lung slice at a pressure state of 20 cmH_2O.

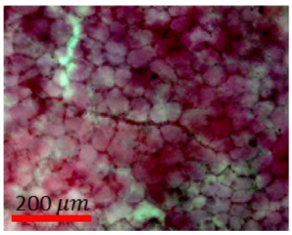

(b) Precision-cut lung slice at a pressure state of 7.5 cmH_2O.

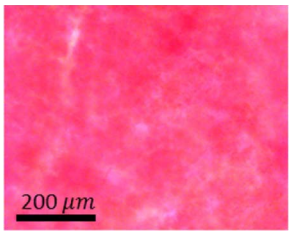

(c) Precision-cut lung slice without gelatin.

Fig. 2. Light microscope images of precision cut lung slices filled at two different pressure states and without filling, respectively.

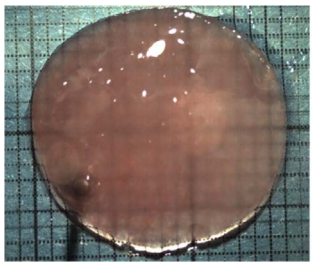

(a) Precision-cut lung slice at 20 cmH_2O pressure state before experiment.

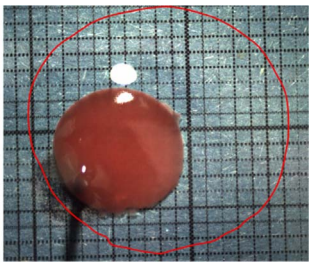

(b) Precision-cut lung slice after experiment. The red line indicates the outline of the sample before the test.

Fig. 3. Volume-pressure-change experiment of one precision-cut lung slice at 20 cmH_2O pressure state.

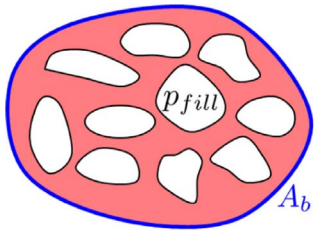

(a) Precision-cut lung slice at certain pressure state p_{fill} before experiment. The blue line indicates the outline of the sample before the test, i.e. the sample area A_b.

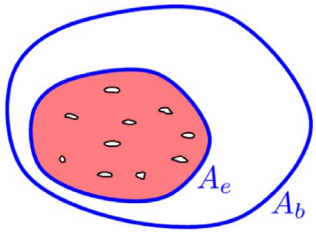

(b) After the experiment the precision-cut lung slice is pressure-free. The outer blue line indicates the sample area before the test A_b and the inner blue line the sample area after the test A_e.

Fig. 4. Sketch of volume-pressure-change experiment. (For interpretation of the references to color in this figure legend, the reader is referred to the web version of this article.)

performed. Experiments were conducted within 48 h after removal of the lung, as previous studies showed that PCLS are viable for at least three days (Martin et al., 1996).

2.2. Volume-pressure-change experiment: experimental set-up

For the volume-pressure-change experiment, each sample was put on a scaled plastic and fixed at one point to prevent it from sliding during the test (Fig. 3a). Above the plastic, a camera monitored the experiment.

A few drops of 37 °C warm MEM were added onto the tissue. Thus, the tissue became warm, and the gelatin melted; as a consequence, the tissue contracted. Due to the foam-like structure of the tissue and because the tissue was stretched, the liquid gelatin was squeezed out of the PCLS (Fig. 3b). If the slices are thin enough, all the gelatin is squeezed out of all alveoli in the PCLS. For example, slices of lung parenchyma filled at a pressure state of p_{fill} = 10 cmH_2O should not be thicker than 2 mm. Otherwise, the gelatin in the inner alveoli is not able to leave the tissue.

The tissue is not damaged during the experiment, as the MEM is 37 °C warm, which is equal to the body-temperature of the rats.

Before the experiment, the gelatin in the tissue was solid; therefore, the PCLS were present at a well-defined pressure state (Fig. 2a and b). Once the gelatin had left the PCLS, the pressure state was dissolved and the tissue returned to its pressure-free state. Fig. 2c depicts a light microscope image of lung parenchyma without gelatin; indeed, the tissue is pressure-free as all alveoli are collapsed. Both pressure states, before and as well after the dissolution of the gelatin, are static. This pressure change lead to a volume change of the PCLS, which was monitored by means of the camera, as indicated in Fig. 3. Video S1 shows the whole experiment in real time.

2.3. Volume-pressure-change experiment: measurements

Sketch 4 illustrates the experiment shown in Fig. 3. As long as the gelatin is solid in the sample a certain pressure state p_{fill}, which is equal to the pressure with which the lungs were filled, acts in the tissue (Fig. 4a). Once the gelatin has melted and left the parenchyma, the stress state is dissolved, and the PCLS is returned to its pressure-free state $p_e = 0$; as a result, the alveoli are closed (Fig. 4b). Accordingly, the pressure change

$$\Delta p = p_{fill} - p_e = p_{fill} := p \tag{1}$$

between the two measured states is equal to the pressure p_{fill} with which the lungs were filled - hereafter, for the sake of simplicity, indicated as the pressure p.

This pressure change p results in a volume change J of the sample. For the quantification of this volume change J, we measured the area of the sample A_b before and the area A_e at the end of the test (blue lines in Fig. 4). The thickness before the experiment d_b of each sample was determined by means of a light microscope (Bel-Brunon et al., 2014). With this set-up, the thickness after the experiment d_e cannot be measured precisely, as the weight of the used glass plate (0.15 g) squeezes the sample, thus, influences the measurement. As long as the gelatin is fixed in the sample, the specimen is thicker, and the gelatin-parenchyma mixture is much stiffer than the parenchyma of the pressure-free PCLS. Hence, the weight of the glass plate does not change the thickness of the sample before the test, but makes it impossible to measure the thickness change accurately. But, since we assume that lung parenchyma is isotropic (Hoppin et al., 1975; Sobin et al., 1988; Toshima et al., 2004), the volume change

Table 1
Sample and rat information of volume-pressure-change experiment. In total, 26 rats and 287 samples were evaluated.

pressure [cmH_2O]	rat number	number of samples	weight [g]
$p = 2.5$	1	10	217.0
$p = 5$	2	5	260.0
$p = 5$	3	7	234.0
$p = 5$	4	8	279.3
$p = 7.5$	5	15	283.7
$p = 7.5$	6	9	282.0
$p = 7.5$	7	12	275.5
$p = 10$	8	7	269.7
$p = 10$	9	19	251.7
$p = 10$	10	9	286.7
$p = 12.5$	11	14	263.5
$p = 12.5$	12	13	230.0
$p = 12.5$	13	9	282.4
$p = 15$	14	18	313.0
$p = 15$	15	12	295.5
$p = 15$	16	7	269.5
$p = 17.5$	17	15	243.0
$p = 17.5$	18	8	261.0
$p = 17.5$	19	13	297.2
$p = 20$	20	6	269.9
$p = 20$	21	10	260.5
$p = 20$	22	13	330.0
$p = 25$	23	13	240.0
$p = 25$	24	12	279.4
$p = 30$	25	13	288.0
$p = 30$	26	10	289.0
	26	287	

$$J = \frac{V_b}{V_e} = \left(\frac{A_b}{A_e}\right)^{\frac{3}{2}} \tag{2}$$

can be calculated from the measured area change. Herein, the relations $J = \lambda^3$ and $\Delta A = \lambda^2$, with λ being the stretch ratio in one direction, are used. The thickness of the pressure-free PCLS $d_e = \frac{d_b}{\lambda}$ is calculated from this area change and used for the uniaxial tension tests (Section 2.4).

We studied a pressure range from 2.5 to 30 cmH_2O because smaller pressure levels cannot be prepared and, at higher pressure levels, the tissue fissured. Furthermore, this pressure range is in accordance with the physiological (Diamond and O'Donnell, 1977) and the higher pathophysiological pressure range. The maximal pressure used during mechanical ventilation (the barotrauma safety margin) is 35 cmH_2O (Uhlig and Uhlig, 2004); this maximum pressure is reduced in the absence of surfactant (Neergaard, 1929; Smith and Stamenovic, 1986).

All samples obtained from one rat have the same pressure change p, and the corresponding volume change J of each sample was measured. For a precise description of the volume-pressure-change relation of lung parenchyma, at each pressure level, samples of 2 or 3 rats were tested (except at 2.5 cmH_2O). Hence, 287 specimens from 26 rats were evaluated, as described in Table 1.

2.4. Uniaxial tension test

The filling of rat lungs with a pressure below 5 cmH_2O is challenging. To also identify the material behavior at small volume changes, uniaxial tension tests were performed. After the volume-pressure-change experiment, the PCLS are pressure-free. With 36 of these pressure-free lung tissue slices, uniaxial tension tests were carried out (Table 2).

Table 2
Number of tested specimens of uniaxial tension test. Rat number refers to the rat information in Table 1. In total, 36 PCLS were examined.

Rat	6	7	10	15	21	24
Number of samples	2	9	6	7	4	8

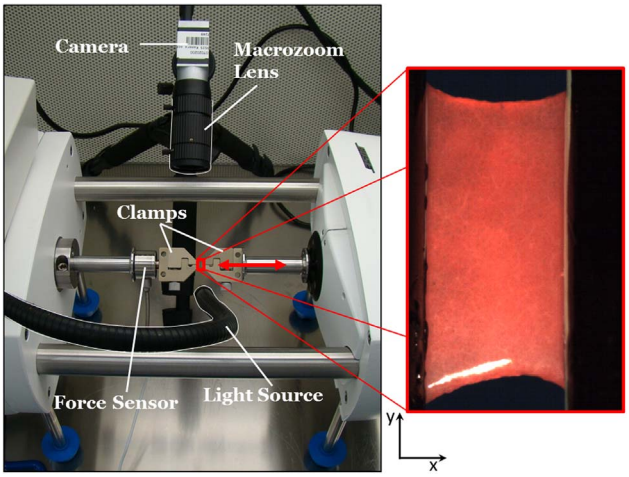

Fig. 5. Experimental set-up of uniaxial tension test with magnified sample. The double arrow indicates the tensile direction.

Since the experimental set-up was described in previous papers by Bel-Brunon et al. (2014) and Rausch et al. (2011) and the uniaxial tension tests were just conducted to complement the information from the volume-pressure-change experiment, only the main features are reiterated here.

Experimental set-up. The specimens were tested using a Bose ElectroForce 3100 uniaxial tension tester (TA Instruments, New Castle, Delaware, USA). The samples were fixed between two clamps that were specifically designed for damage-free and sliding-free use with PCLS. The internal displacement sensor of the machine (range of ± 2.5 mm with a resolution of 12.5 µm) and a force sensor (range of ± 0.5 N with a resolution of 2.5 mN) were connected to the clamps. To calculate the displacement field, a camera with a macrozoom lens (frame rate $100\frac{\text{frames}}{\text{s}}$, resolution 800 × 1000 pixels), which was placed perpendicular to the sample plane, recorded the test (Fig. 5).

The tissue point in which the sample was fixed during the volume-pressure-change experiment was either located in the clamps or cut off before the test. Consequently, the tested tissue area was always damage-free.

Performing our experiments at room temperature instead of body temperature has no effect on the mechanical properties because, as shown in a study by Karlinsky et al. (1985), the mechanical behavior of lung tissue does not change significantly between 10 °C and 50 °C.

Testing protocol. The initial length of the test domain of the specimen was exactly $l_0 = 1.8$ mm. The tissue was loaded for preconditioning and testing with sinusoidal oscillations, as this mimics the physiological behavior during the breathing cycles. We performed oscillations with an amplitude of 1.25 mm, a start value of $l_0 + 0.4$ mm and a frequency of 0.2 Hz. 9 cycles were conducted for the preconditioning, while the ascending part of the 10th cycle was used for the actual testing of the hyperelastic material behavior.

Image registration. The present work focuses on the compressible material behavior. Therefore, we were particularly interested in the width of the sample in addition to the force and displacement measurements. For this reason, the two-dimensional deformation field in space and time was determined by means of an image registration, as described in a previous paper by Bel-Brunon et al. (2014).

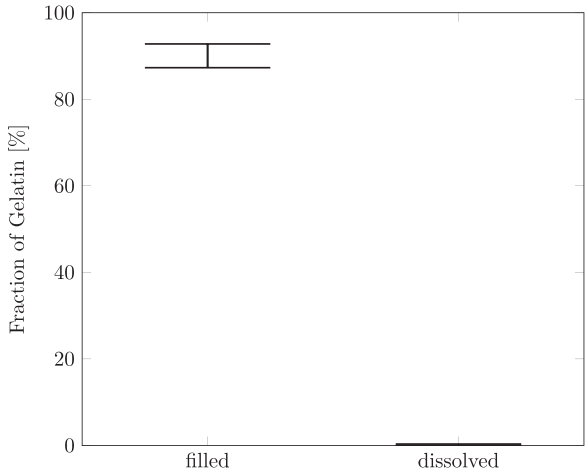

Fig. 6. Gelatin in the PCLS before and after dissolution with a 37 °C warm medium (n = 4).

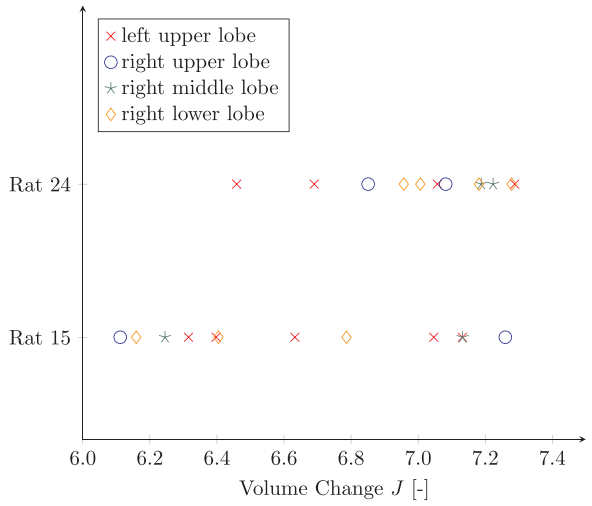

Fig. 7. No significant difference between volume-change measurements in different lobes. Data exemplary shown for rat 15 (p = 15 cmH_2O) and rat 24 (p = 25 cmH_2O).

3. Experimental results

Before the experimentally measured volume-pressure-change relation is shown, various assumptions underlying the volume-pressure-change experiment were examined.

3.1. Proof of assumption of pressure-free state

It is assumed that the PCLS are gelatin-free and, as a consequence, also pressure-free at the end of the volume-pressure-change experiment. To demonstrate the validity of this assumption, we determined the remaining gelatin with the help of weight measurements.

For these weight measurements, the preparation of the PCLS was modified. After the chest was opened, first, the lungs together with the heart and trachea were removed from the rat body, and their weight was measured. Second, the lungs were filled with gelatin, as described in Section 2.1, and their weight was measured again. Third, the heart and the trachea were removed, and the weight was measured again. Hence, the percentage weight of the gelatin on the whole weight of the gelatin-lung was determined. Next, the PCLS were further prepared normally, as explained in Section 2.1, and the weight of the PCLS was measured. Lastly, the gelatin was removed with a 37 °C warm medium, as described in Section 2.2. With the determination of the weight of these PCLS, it was possible to calculate the percentage of gelatin in the lung slices after the experiment.

Fig. 6 displays the percentage of gelatin in isolated tissue before (filled) and after (dissolved) the dissolution of the gelatin. In summary, 0.044 ± 0.12% gelatin remained in the dissolved tissue. This data shows that the gelatin completely (i.e., the remaining proportion is not significant to zero) left the PCLS during the volume-pressure-change experiment; in conclusion, the tissue is pressure-free after the experiment.

3.2. Difference of measurements between lobes

During the preparation described in Section 2.1, each rat lung was filled by means of a gelatin column. The different areas of the lung were loaded with a similar height of the gelatin column, because during the preparation the rat was lying. Consequently, we assume that the lungs were filled homogeneously; hence, in each lung slice, the same pressure acts, and, for all samples of one rat, the same volume change can be measured, except for physiological variations. To verify this assumption, we separated the slices of two rats with respect to their lobes. Samples were prepared from all three right lobes and the left upper lobe.

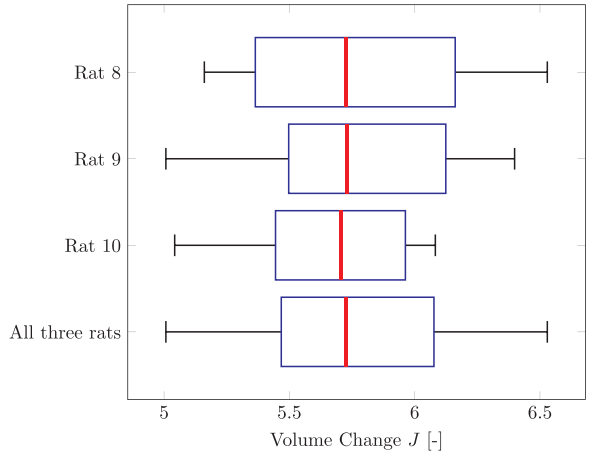

Fig. 8. No significant difference between measurements of lungs of different rats filled at the same pressure of 10 cmH_2O.

Fig. 7 shows the measured volume changes of specimens of rat 15, which was filled at a pressure of 15 cmH_2O, and of rat 24, which was filled at 25 cmH_2O. The figure illustrates the normal physiological difference between the measurements of different samples. Further, it can be seen that no significant difference between the volume change of specimens of different lobes can be measured. Hence, all lobes of one lung are filled with the same pressure and the filling is homogeneous. In conclusion, it is valid to assume that the same pressure acts in all tissue slices of one rat.

3.3. Difference of measurements between different rats

Next, we studied whether a difference between the measurements of samples from different rats exists. Fig. 8 displays the volume-change data of three different rats, all filled at the same pressure of 10 cm H_2O, and the measurements of all three rats in one boxplot. The normal physiological difference between the data of different specimens is visible for each rat. In contrast, no significant difference in the measured volume change can be observed between the rats. Indeed, for the chosen pressure, the median values of the three rats are remarkably similar.

Not only at a pressure of 10 cmH_2O no difference between the volume change of different rats exist; in fact, at all pressure levels, no

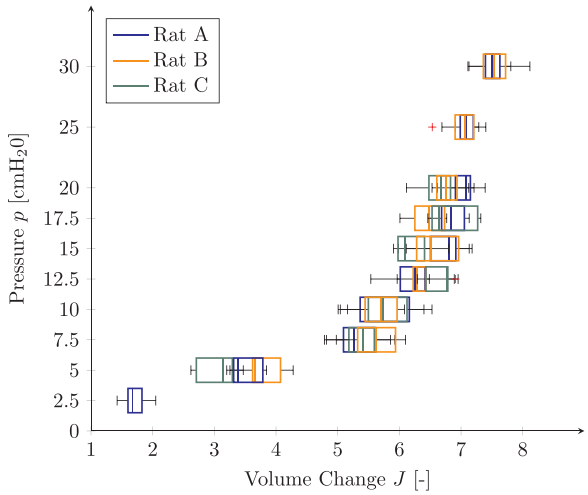

Fig. 9. No significant difference between measurements of lungs of different rats filled at the same pressure. To show the difference at the same pressure level, the boxplot color of the rats at the same pressure level are alternated. Rats A, B and C denote the first, second and third rat at this pressure level.

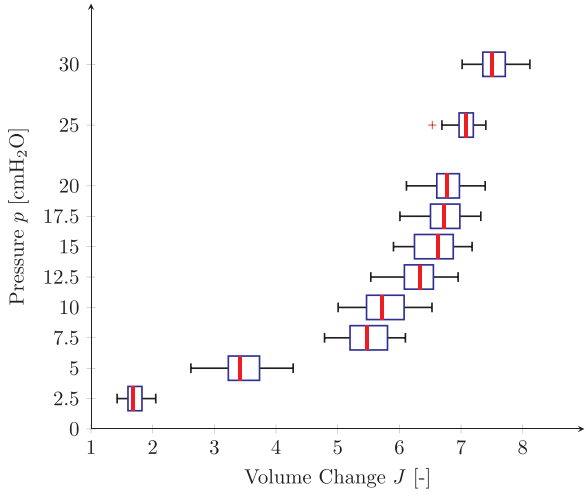

Fig. 10. Experimental result of volume-pressure-change experiment.

significant difference between the data of different rats were observed. To illustrate this, Fig. 9 displays the measurements of each rat in a separate boxplot. To show the difference between the rats, the colors of the boxplot are alternated at each pressure level.

In summary, we observed no significant difference between samples from different rats filled at the same pressure. Hence, it is valid to treat all samples filled at the same pressure level equally.

3.4. Experimentally measured volume-pressure-change relation

After having validated the underlying assumptions of the volume-pressure-change experiments, the results of our measurements are presented in the following. All samples of rats filled at the same pressure level can be treated equally; accordingly, in Fig. 10, these samples are summarized in one boxplot. In total, we examined 287 PCLS from 26 rats (Table 1).

Fig. 10 illustrates the volume-pressure-change behavior of lung parenchyma with a pressure change from 2.5 to 30 cmH$_2$O. The pressure 2.5 cmH$_2$O is represented by just 10 samples of only one rat, and this pressure is challenging in preparation. Hence, at this pressure the

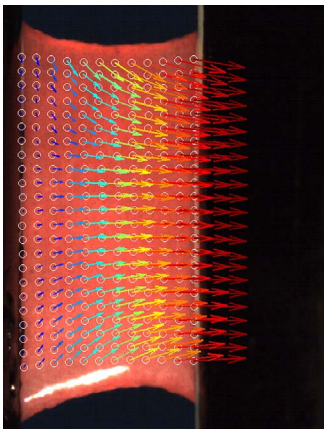

Fig. 11. Full, two-dimensional displacement field of sample during uniaxial tension test.

determined volume-change data is probably error-prone and not entirely reliable; for this reason, we conducted additional uniaxial tension tests (see Section 3.5 for results).

Apart from the lowest pressure level, we examined at least 20 samples of at least 2 rats at all the other pressure levels. Consequently, the volume-change data corresponding to the pressures 5–30 cmH$_2$O is reliable for the description of the material behavior.

The highest meaningful pressure for this experiment is 30 cmH$_2$O. First, higher pressures are only physiological for a short time-frame during deep inspiration; second, a static filling pressure of 30 cmH$_2$O caused leaks in some preparations and these lungs could not be used for the experiments. Here, only those samples for which we were able to determine a static pressure of 30 cmH$_2$O in the tissue are shown.

The measured volume-pressure-change data in Fig. 10 illustrates the nonlinear volume-pressure-change behavior of lung parenchyma over the whole physiological range, especially also for high volume changes. Whereas a small pressure change is needed to achieve a certain volume change up to a pressure level of 7.5 cm H$_2$O, the material behaves much stiffer at higher pressure levels, as much higher pressure changes are required for the same volume change. Hence, the compressible material behavior of lung parenchyma is nonlinear, dependent on the occurring pressure level.

3.5. Volume-pressure-change relation in uniaxial tension tests

The information of the volume-pressure-change experiment at small pressure changes is only represented by few samples. Accordingly, we enhance the description of the material behavior at low volume changes by conducting uniaxial tension tests combined with a deformation field measurement. The volume change achievable in uniaxial tension tests is below 2; hence, this information is beneficial for the description of the volume-pressure-change measurements below a pressure of 5 cmH$_2$O. The uniaxial tension test setup is described in Section 2.4 and in Bel-Brunon et al. (2014) and Rausch et al. (2011). During the uniaxial tension test not only the force and displacement were measured by the testing machine, but additionally images of the sample during the test were recorded. The full two-dimensional displacement field of each sample is reconstructed using image registration techniques. Fig. 11 shows the displacement field of one sample at one exemplary time step. To calculate the compressible material behavior this heterogeneous displacement field is utilized in the inverse analysis of the tension test (see Section 4.2). As a consequence, no assumptions regarding the stress or strain field in the sample are necessary for the material identification.

4. Identification of a compressible material model

The presented experimental measurements enabled us to identify a phenomenological, hyperelastic strain-energy function to describe the compressible material behavior of lung parenchyma. Although a hyperelastic strain-energy function describes volumetric and isochoric deformations, the aim of this paper is the identification of the volumetric material behavior of lung parenchyma; hence, the focus of the identification are the volume-pressure-change measurements, and the uniaxial tension tests are just used to determine precise start values in the regime of small volume changes. In the case of purely volumetric deformation, the strain-energy function can be completely described by means of a volume-pressure-change relation. In the following, the general framework of the identification is provided and applied for one suitable strain-energy function.

4.1. Constitutive law and pressure-volume-change relation

As mentioned above, lung parenchyma is commonly assumed to be an isotropic material. Therefore, a hyperelastic strain-energy function

$$\Psi(I_1, I_2, I_3) \tag{3}$$

with the invariants of the right Cauchy-Green deformation tensor

$$I_1 = \mathrm{tr}\mathbf{C} \tag{4a}$$

$$I_2 = \frac{1}{2}[(\mathrm{tr}\mathbf{C})^2 - \mathrm{tr}(\mathbf{C})^2] \tag{4b}$$

$$I_3 = \det \mathbf{C} = J^2 \tag{4c}$$

is utilized to describe the elastic behavior of lung parenchyma. In our volume-pressure-change experiment a purely volumetric deformation occurs; hence, the deformation gradient

$$\mathbf{F}_{vol} = \begin{pmatrix} \lambda & 0 & 0 \\ 0 & \lambda & 0 \\ 0 & 0 & \lambda \end{pmatrix} \tag{5}$$

can be simplified, with λ being the stretch. Accordingly, the volume change

$$J = \lambda^3 = \frac{V_b}{V_e} \tag{6}$$

is equal to the measured volume change in Section 2.3, and the invariants

$$I_1^{vol} = 3J^{\frac{2}{3}} \tag{7a}$$

$$I_2^{vol} = 3J^{\frac{4}{3}} \tag{7b}$$

$$I_3^{vol} = J^2 \tag{7c}$$

are formulated as a function of this volume change J. Consequently, the strain-energy function

$$\Psi(I_1^{vol}, I_2^{vol}, I_3^{vol}) = \Psi_{vol}(3J^{\frac{2}{3}}, 3J^{\frac{4}{3}}, J^2) = \Psi_{vol}(J) \tag{8}$$

can be reformulated for purely volumetric deformation. In this purely volumetric case, the stress-strain behavior can be fully described with a volume-pressure-change relation. Therefore, the hydrostatic pressure

$$p = \frac{\partial \Psi_{vol}}{\partial J} \tag{9}$$

is derived from the strain-energy function (Holzapfel, 2010). For instance, the strain-energy function

$$\Psi(I_1, I_3) = c(I_1 - 3) + \frac{c}{\beta}(I_3^{-\beta} - 1) + c_d(I_1 - 3)^d \tag{10}$$

results in the volume-pressure-change relation

$$p = 2c\left(J^{-\frac{1}{3}} - J^{-2\beta-1}\right) + 2c_d d J^{-\frac{1}{3}}\left(3J^{\frac{2}{3}} - 3\right)^{d-1}. \tag{11}$$

This strain-energy function is suitable to describe our measurements; hence, it will be used in Section 4.3 to identify the volumetric material behavior.

4.2. Methods for the identification of the constitutive parameters

For the determination of the constitutive parameters, a separate identification method was applied for each experiment.

To improve the quality of the fit in the linear region of the volume-pressure-change curve, we used the measurements of the uniaxial tension tests for the identification of the corresponding material parameters $\hat{\mathbf{x}} = [c, \beta]$ of the material model (10). For this purpose, an inverse analysis as described in Bel-Brunon et al. (2014) and Rausch et al. (2011) was performed. Briefly, each uniaxial tension test was simulated with Finite Elements (3D) using the corresponding realistic geometry and the Neumann boundary condition σ_j (derived from the measured forces). The Levenberg-Marquardt algorithm (Levenberg, 1944; Marquardt, 1963) was utilized to minimize the objective function

$$\chi_{\mathrm{uniax}} = \sum_{j=1}^{m} (\mathbf{u}^{\mathrm{mod}}(\mathbf{x}, \sigma_j) - \mathbf{u}_j^{\mathrm{exp}})^2, \tag{12}$$

where m is the number of considered specimens, as listed in Table 2, $\mathbf{u}_j^{\mathrm{exp}}$ is the experimentally measured displacement field (in space and time), and $\mathbf{u}^{\mathrm{mod}}$ is the displacement field predicted by the material model. For each sample j, one set of material parameters $\mathbf{x}$ was identified, but just the material parameters $\hat{\mathbf{x}}$ were further used. Due to assumed isotropy of lung parenchyma, the comparison of the two-dimensional displacement fields is sufficient to fit the three-dimensional material model. Finally, the medians of these material parameters were used as start values for the fit of the measurements of the volume-pressure-change experiment.

Given the determined volume-pressure-change data $[p_i^{\mathrm{exp}}, J_i]$ for each sample i, the nonlinear least-square algorithm lsqcurvefit in MATLAB (R2015b, The MathWorks, Inc., Natick, Massachusetts, USA) was used to minimize the objective function

$$\chi_{\mathrm{vol}} = \sum_{i=1}^{n} (p^{\mathrm{mod}}(\mathbf{x}, J_i) - p_i^{\mathrm{exp}})^2, \tag{13}$$

where n is the number of considered data points listed in Table 1. Further, p^{mod} are the corresponding pressure values predicted by the constitutive model, respective by the derived volume-pressure-change relation (11) and $\mathbf{x} = [c, \beta, c_d, d]$ denotes the vector of model parameters identified. Note that only integers are valid for the parameter d.

In conclusion, we identified the medians of the constitutive parameters $\hat{\mathbf{x}} = [c, \beta]$ that are responsible for the material behavior at small volume changes, by means of inverse analyses of the uniaxial tension tests, and used these separately identified parameters as start values for the final least-square-fit of the volume-pressure-change experiment. This way, the material parameters $\mathbf{x} = [c, \beta, c_d, d]$ were identified.

With this procedure, material parameters not resulting in polyconvex materials could be identified. According to Ball (1976), a polyconvexity condition of the strain-energy function ensures existence

Table 3
Identified constitutive parameters. Start = set of parameters obtained based on inverse analyses of uniaxial tension tests (median results), used as start values for volume-pressure-change experiment identification. Final = final identified constitutive parameters.

parameter	c [Pa]	β	c_d [Pa]	d	NRMSD
start	386.61	1.4738			0.0569
final	286.61	1.1738	0.008238	6	0.1284

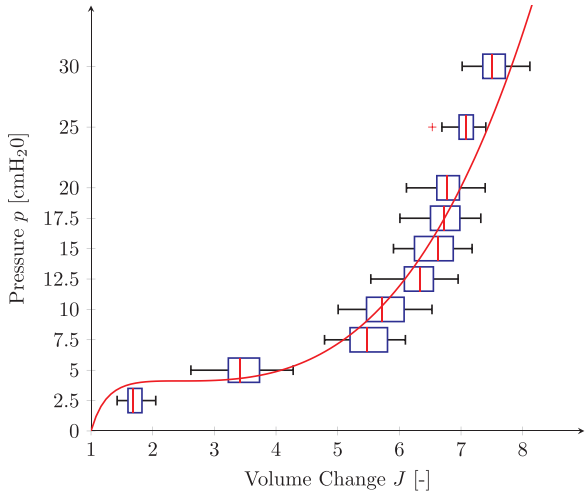

Fig. 12. Identified compressible material model (solid line) superimposed with experimental results.

and uniqueness of the solution. Consequently, the bounds of admissable parameters were adapted iteratively until the identified material satisfied the polyconvexity condition.

To evaluate the accuracy of both fits, we provide the normalized root-mean-square deviation

$$\text{NRMSD} = \frac{\sqrt{\sum_{k=1}^{l} (y^{\text{mod}} - y_k^{\text{exp}})^2}}{\sqrt{l}\,(y_{\text{max}}^{\text{exp}} - y_{\text{min}}^{\text{exp}})}, \tag{14}$$

where y_k represents the displacement $\mathbf{u}_j$, respectively, the pressure p_i. To compare the different data sets, the residuum was normalized by means of the square root of the number of data points l and the experimental data range.

4.3. Identified material parameters

With this strategy, the constitutive parameters of the suitable strain-energy function (10) were identified and are provided in Table 3. The start parameters were identified by means of the inverse analyses of the uniaxial tension tests (parameters are the medians of the identified parameters of all samples). The final parameters were fitted with the measurements of the volume-pressure-change experiments. The volume-change data of the pressure 2.5 cmH$_2$O were not used, as the uniaxial tension test information is more reliable in this regime. The normalized root-mean-square deviation of the fit of the volume-pressure-change measurements is shown in the same line as the final parameters in Table 3.

The identified material model superimposed with the experimental results of the volume-pressure-change experiment is provided in Fig. 12. This figure clearly shows the S-shape of the volume-pressure curve. This shape can be explained by the following observations; first, in the uniaxial tension test, a stiffer behavior was measured; hence, a steep volume-pressure-change relation is necessary in the regime of small volume changes. Second, in the volume-pressure-change experiment, we measured a plateau-like behavior around the pressure of 5 cmH$_2$O; third, above the pressure of 7.5 cmH$_2$O, the material behaved stiff again.

5. Discussion

This paper presents a novel experimental method to measure the volume-pressure-change relation of lung parenchyma; in addition, corresponding experimental results for 287 samples from 26 rats are provided. To describe the measured volume-pressure-change relation, a suitable strain-energy function was chosen, and the corresponding material parameters identified.

To the best of the authors knowledge, this newly derived volume-pressure-change experiment is the first experimental method that enables the measurement of the material behavior of lung parenchyma at high physiological volume changes without any biasing preparation technique, such as freezing of the tissue, as in Hoppin et al. (1975). Hence, in our experiment the tissue is still viable while the material behavior at high volume changes is examined.

During preparation, the parenchyma was filled with gelatin. Thus, no surfactant-air-interaction could occur, and the surfactant was washed out during the experiment. Consequently, the obtained measurements describe the mechanical behavior of the tissue alone, and we do not measure any effect due to surfactant. Indeed, the identified tissue mechanics model can be combined with existing surfactant models (e.g., Wiechert et al., 2009) in a straightforward way. Further, influences of the organ (geometry effects) are excluded, as the mechanical behavior of lung parenchyma is examined with the help of excised samples. Other constituents (e.g., large airways or vessels) can be included in the computational lung model (e.g., Roth et al., 2017). To also describe the mechanical effect of small airways, the experiments could be conducted with tissue samples that contain parenchyma and small airways.

The validity of the underlying assumptions of the volume-pressure-change experiments have been shown. First, the assumption that the tissue is gelatin-free (hence, pressure-free) after the experiment is justified, as described in Section 3.1. Second, the filling of the lungs is homogeneous, as the samples of different rats behave similarly, as demonstrated in Sections 3.2 and 3.3. Consequently, it is valid to treat all samples excised from lungs with the same filling pressure equally.

Finally, we calculate the volume change from the measured area change. The weight of the used glass plate influences the measurement of the thickness change, and the volume of the pressure-free specimens is too low to measure it in a water displacement experiment. For example, the volume of a gelatin-free PCLS (rat 13) is approximately 50 mm^3, which is equal to a water displacement of just 0.05 ml. The calculation of the volume change from the measured area change is justified since we assume isotropy of lung parenchyma. This assumption is state of the art (e.g., Hoppin et al., 1975; Sobin et al., 1988; Toshima et al., 2004) and is also supported by our experimental data. Since the orientation of the samples with respect to the lung is random, we would expect a much higher scatter of the measured data in case of a pronounced anisotropy of lung parenchyma. Since this is not the case, the assumption of isotropy seems to be justified.

In the present work, the measured volume-pressure-change relation of lung parenchyma of the whole physiological and the pathophysiological range is provided. We measured a factor for the volume change from 3 to 4 (according to a pressure of 5 cmH$_2$O), up to 7–8 (according to a pressure of 30 cmH$_2$O), which is in agreement with the physiological volume change factor of 3–10 for human lungs on the organ scale (Agostoni and Hyatt, 2011).

The measurements of the volume-pressure-change experiment (Fig. 10) express the volumetric material behavior up to the maximum physiological achievable pressure changes. For each pressure level, the corresponding volume change is precisely described, as at least 20 samples of at least 2 different rats were measured at each pressure level. Moreover, the volumetric material description was enhanced in the

regime of small volume changes through information from the uniaxial tension tests. In conclusion, this is the first study that provides precise experimental results of the volumetric material behavior of lung parenchyma over the whole physiological range.

In addition, this paper presents a suitable hyperelastic compressible material model of lung parenchyma with parameters identified from the experimental results. Since the focus of this paper is the novel experimental technique and the experimental results, we present the general procedure for the parameter identification by means of one exemplary strain-energy function. Although this strain-energy function and the determined constitutive parameters are able to represent the material behavior well, the proposed approach is by no means restricted to this particular constitutive model.

In this study, the volumetric material behavior of lung parenchyma is measured and identified because lung tissue is mainly subjected to volumetric deformations during breathing and mechanical ventilation; however, non-symmetric extensions or small isochoric deformations also occur. Thus, a possible improvement of the presented identification method would be to use the information of the uniaxial tension tests not only for the determination of the start values for the identification of the volumetric material behavior, but also to identify the isochoric information of the uniaxial tension tests. This will allow us to identify a hyperelastic material model that describes not only the dominating volumetric material behavior, but also small isochoric deformations or more complex strain states (for example, in diseased, heterogeneous lungs).

In this paper, an elastic material model is derived; however, lung parenchyma is viscoelastic, as are most biological tissues (Bel-Brunon et al., 2014). In the volume-pressure-change experiment, static pressure levels were compared, and the development of the internal pressure is not measurable during the experiment, but, in the uniaxial tension test, viscoelastic effects could be determined. Hence, in the future, a possible extension of the nonlinear hyperelastic material model would be the use of the viscoelastic information of the uniaxial tension tests to model the viscoelastic material behavior. Accordingly, this study is a first step towards a viscohyperelastic material model that describes all possible deformations of lung parenchyma.

6. Conclusion

This study presents the first experimental methods to measure the volumetric material behavior of lung parenchyma over the whole physiological and pathophysiological range, especially at high pressure respective volume changes. To the best of our knowledge, previously, only Hoppin et al. (1975) experimentally determined the volumetric material behavior of lung parenchyma. However, their study had some major limitations, as mentioned in the introduction, which are overcome in our novel experiment.

The measured and identified nonlinear compressible material model will allow us to perform finite element simulations of lung parenchyma, and this model will be included in our different computational lung models. The simulations of this overall lung model can be compared with measurements on the whole lung to enable the in-vivo validation of our model. In the future, this material model will help to quantify the stresses and strains of lung parenchyma during normal and artificial breathing.

Acknowledgment

We gratefully acknowledge the technical assistance of Hanna Czajkowska.

Appendix A. Supplementary data

Supplementary data associated with this article can be found in the online version at http://dx.doi.org/10.1016/j.jmbbm.2017.08.001.

References

Agostoni, E., Hyatt, R.E., 2011. Static Behavior of the Respiratory System. In: Comprehensive Physiology. John Wiley & Sons, Inc..

Andrikakou, P., Vickraman, K., Arora, H., 2016. On the behaviour of lung tissue under tension and compression. Sci. Rep. 6. http://dx.doi.org/10.1038/srep36642.

Ball, J.M., 1976. Convexity conditions and existence theorems in nonlinear elasticity. Arch. Ration. Mech. Anal. 63, 337–403. http://dx.doi.org/10.1007/BF00279992.

Bel-Brunon, A., Kehl, S., Martin, C., Uhlig, S., Wall, W.A., 2014. Numerical identification method for the non-linear viscoelastic compressible behavior of soft tissue using uniaxial tensile tests and image registration Application to rat lung parenchyma. J. Mech. Behav. J. Mech. Behav. 29, 360–374. http://dx.doi.org/10.1016/j.jmbbm.2013.09.018.

Berger, L., Bordas, R., Burrowes, K., Grau, V., Tavener, S., Kay, D., 2015. A poroelastic model coupled to a fluid network with applications in lung modelling. Int. J. Numer. Method. Biomed. Eng. 32. http://dx.doi.org/10.1002/cnm.2731.

Budiansky, B., Kimmel, E., 1987. Elastic moduli of lungs. J. Appl. Mech. 54, 351–358. http://dx.doi.org/10.1115/1.3173019.

Consensus-Conference, 1999. International Consensus Conferences in Intensive Care Medicine: Ventilator-associated Lung Injury in ARDS. Am. J. Respir. Crit. Care Med. 160, 2118–2124 http://dx.doi.org/10.1164/ajrccm.160.6.ats16060.

Denny, E., Schroter, R., 2000. Viscoelastic behavior of a lung alveolar duct model. J. Biomech. Eng. 122, 143–151. http://dx.doi.org/10.1115/1.429644.

Diamond, L., O'Donnell, M., 1977. Pulmonary mechanics in normal rats. J. Appl. Psychol. 43, 942–948.

Gao, J., Huang, W., Yen, R., 2005. Mechanical properties of human lung parenchyma. Biomed. Sci. Instrum. 42, 172–180.

Holzapfel, G.A., 2010. Nonlinear Solid Mechanics - A Continuum Approach for Engineering. John Wiley & Sons Ltd., Chichester, England.

Hoppin, F., Lee, G., Dawson, S., 1975. Properties of lung parenchyma in distortion. J. Appl. Psychol. 39, 742–751.

Karlinsky, J.B., Bowers, J.T., Fredette, J.V., Evans, J., 1985. Thermoelastic properties of uniaxially deformed lung strips. J. Appl. Psychol. 58, 459–467.

Lai-Fook, S.J., 1977. Lung parenchyma described as a prestressed compressible material. J. Biomech. 10, 357–365. http://dx.doi.org/10.1016/0021-9290(77)90008-2.

Lai-Fook, S.J., Wilson, T.A., Hyatt, R.E., Rodarte, J.R., 1976. Elastic constants of inflated lobes of dog lungs. J. Appl. Psychol. 40, 508–513.

Lanir, Y., 1983. Constitutive equations for the lung tissue. J. Biomech. Eng. 105, 374–380. http://dx.doi.org/10.1115/1.3138435.

Levenberg, K., 1944. A method for the solution of certain problems in least squares. Q. Appl. Math. 2, 164–168.

Maksym, G.N., Bates, J.H., 1997. A distributed nonlinear model of lung tissue elasticity. J. Appl. Psychol. 82, 32–41.

Marquardt, D.W., 1963. An algorithm for least-squares estimation of nonlinear parameters. SIAM J. Appl. Math. 11, 431–441. http://dx.doi.org/10.1137/0111030.

Martin, C., Uhlig, S., Ullrich, V., 1996. Videomicroscopy of methacholine-induced contraction of individual airways in precision-cut lung slices. ERJ Open Res. 9, 2479–2487.

Navajas, D., Maksym, G.N., Bates, J., 1995. Dynamic viscoelastic nonlinearity of lung parenchymal tissue. J. Appl. Psychol. 79, 348–356.

v. Neergaard, K., 1929. Neue Auffassungen über einen Grundbegriff der Atemmechanik. Ges. Exo. Med. 66, 373–394 http://dx.doi.org/10.1007/bf02621963›.

Rausch, S.M., Martin, C., Bornemann, B., Uhlig, S., Wall, W.A., 2011. Material model of lung parenchyma based on living precision-cut lung slice testing. J. Mech. Behav. J. Mech. Behav. 4, 583–592. http://dx.doi.org/10.1016/j.jmbbm.2011.01.006.

Roth, C.J., Yoshihara, L., Ismail, M., Wall, W.A., 2017. Computational modelling of the respiratory system: discussion of coupled modelling approaches and two recent extensions. Comput. Methods Appl. Mech. Eng. 314, 473–493. http://dx.doi.org/10.1016/j.cma.2016.08.010.

Smith, J.C., Stamenovic, D., 1986. Surface forces in lungs. I. Alveolar surface tension-lung volume relationships. J. Appl. Psychol. 60, 1341–1350.

Sobin, S.S., Fung, Y.C., Tremer, H.M., 1988. Collagen and elastin fibers in human pulmonary alveolar walls. J. Appl. Psychol. 64, 1659–1675.

Stamenovic, D., Yager, D., 1988. Elastic properties of air- and liquid-filled lung parenchyma. J. Appl. Psychol. 65, 2565–2570.

Tai, R.C., Lee, G.C., 1981. Isotropy and homogeneity of lung tissue deformation. J. Biomech. 14, 243–252. http://dx.doi.org/10.1016/0021-9290(81)90069-5.

Toshima, M., Ohtani, Y., Ohtani, O., 2004. Three-dimensional architecture of elastin and collagen fiber networks in the human and rat lung. Arch. Histol. Cytol. 67, 31–40. http://dx.doi.org/10.1679/aohc.67.31.

Uhlig, S., Uhlig, U., 2004. Pharmacological interventions in ventilator-induced lung injury. Trends Pharmacol. Sci. 25, 592–600. http://dx.doi.org/10.1016/j.tips.2004.09.002.

Vawter, D., Fung, Y., West, J., 1978. Elasticity of excised dog lung parenchyma. J. Appl. Psychol. 45, 261–269.

Wall, W.A., Wiechert, L., Comerford, A., Rausch, S., 2010. Towards a comprehensive

computational model for the respiratory system. Int. J. Numer. Method. Biomed. Eng. 26, 807–827. http://dx.doi.org/10.1002/cnm.1378.
Ware, L.B., Matthay, M.A., 2000. The acute respiratory distress syndrome. N. Engl. J. Med. 342, 1334–1349. http://dx.doi.org/10.1056/NEJM200005043421806.
Wiechert, L., Metzke, R., Wall, W.A., 2009. Modeling the mechanical behavior of lung tissue at the microlevel. J. Eng. Mech. -ASCE 135, 434–438. http://dx.doi.org/10.1061/(ASCE)0733-9399(2009)135:5(434).
Yager, D., Feldman, H., Fung, Y.C., 1992. Microscopic vs. macroscopic deformation of the pulmonary alveolar duct. J. Appl. Psychol. 72, 1348–1354.
Yoshihara, L., Roth, C.J., Wall, W.A., 2017. Fluid-structure interaction including volumetric coupling with homogenised subdomains for modeling respiratory mechanics. Int. J. Numer. Methods Biomed. Eng. 33. http://dx.doi.org/10.1002/cnm.2812.
Yuan, H., Kononov, S., Cavalcante, F.S., Lutchen, K.R., Ingenito, E.P., Suki, B., 2000. Effects of collagenase and elastase on the mechanical properties of lung tissue strips. J. Appl. Psychol. 89, 3–14.